Published October 5, 2017

Journal of Environmental Quality DATASETS

# A Dataset for Three-Dimensional Distribution of 39 Elements Including Plant Nutrients and Other Metals and Metalloids in the Soils of a Forested Headwater Catchment

B. Wu,* I. Wiekenkamp, Y. Sun, A. S. Fisher, R. Clough, N. Gottselig, H. Bogena, T. Pütz, N. Brüggemann, H. Vereecken, and R. Bol

## Abstract

Quantification and evaluation of elemental distribution in forested ecosystems are key requirements to understand element fluxes and their relationship with hydrological and biogeochemical processes in the system. However, datasets supporting such a study on the catchment scale are still limited. Here we provide a dataset comprising spatially highly resolved distributions of 39 elements in soil profiles of a small forested headwater catchment in western Germany (http://teodoor.icg.kfa-juelich.de/ibg3searchportal2/dispatch?searchparams=freetext-Wuestebach&metadata.detail.view.id=7d37ae00-20f6-408e-8660-33bfba07c869) to gain a holistic picture of the state and fluxes of elements in the catchment. The elements include both plant nutrients and other metals and metalloids that were predominately derived from lithospheric or anthropogenic inputs, thereby allowing us to not only capture the nutrient status of the catchment but to also estimate the functional development of the ecosystem. Soil samples were collected at high lateral resolution ($\leq$60 m), and element concentrations were determined vertically for four soil horizons (L/Of, Oh, A, B). From this, a three-dimensional view of the distribution of these elements could be established with high spatial resolution on the catchment scale in a temperate natural forested ecosystem. The dataset can be combined with other datasets and studies of the TERENO (Terrestrial Environmental Observatories) Data Discovery Portal (http://teodoor.icg.kfa-juelich.de/ibg3searchportal2/index.jsp) to reveal elemental fluxes, establish relations between elements and other soil properties, and/or as input for modeling elemental cycling in temperate forested ecosystems.

## Core Ideas

- A dataset of elemental concentrations for four soil horizons of a forested catchment
- Highly linked with a previous dataset on lateral and vertical distribution of nutrients
- The dataset can be used to explore biogeochemical elements and their fluxes in natural soil systems

Elemental cycling in terrestrial ecosystems involves various soil biogeochemical processes and fluxes that are controlled by soil chemical and physical properties. The source of elements in soils can be derived from the lithosphere through weathering of the parent materials, evolved in pedogenic processes, and/or through anthropogenic activities. Continuous weathering of parent materials leads to dissolution, hydration, hydrolysis, oxidation, reduction, and carbonization of elements that subsequently participate in pedogenic processes forming secondary minerals that are relatively stable and equilibrated with a particular soil environment (Kabata-Pendias and Mukherjee, 2007). With changing soil conditions, such as those caused by seasonal waterlogging or deforestation, these minerals may become unstable and involved in leaching, adsorption, and precipitation processes. Some of the elements become available to plants in their dissolved or organically bound forms. Others, however, may become immobilized and accumulate in the soil. The majority of elements in the soil show a lithospheric character, showing preference of binding with oxygen. However, many elements are also concentrated in silicates, carbonates, phosphates, and sulfates (Sigel and Sigel, 2003).

Diverse soil characteristics and factors such as geomorphology and vegetation result in spatially and temporally heterogeneous distribution of elements in the soil. Vertical and lateral transportation and transformation of the elements are highly related to the physical and chemical factors of abiotic systems, as well as to living organisms. Fast development of analytical techniques has resulted in an increase of the number of studies on element content and speciation in terrestrial systems during the last three decades (Kabata-Pendias and Szteke, 2015). Most of the elements across the periodic table have been explored with respect to their biogeochemical behaviors in terrestrial and aquatic systems, and the investigation of nutrients and pollutant elements is of particular interest.

Spatial distribution of an element can reflect its cycling during soil formation and utilization. Despite our knowledge



J. Environ. Qual. 46:1510–1518 (2017).
doi:10.2134/jeq2017.05.0193
Supplemental material is available online for this article.
Received 9 May 2017.
Accepted 5 Sept. 2017.
*Corresponding author (b.wu@fz-juelich.de).

B. Wu, I. Wiekenkamp, Y. Sun, N. Gottselig, H. Bogena, T. Pütz, N. Brüggemann, H. Vereecken, and R. Bol, Institute of Bio- and Geosciences: Agrosphere (IBG-3), Forschungszentrum Jülich GmbH, 52425 Jülich, Germany; A.S. Fisher and R. Clough, School of Geography, Earth and Environmental Sciences, Faculty of Science and Engineering, Plymouth Univ., Plymouth PL4 8AA, UK. Assigned to Associate Editor Budong Qian.

**Abbreviations**: HRE, second group of the rare earth elements from terbium to lutetium; ICP–MS, inductively coupled plasma mass spectrometry; ICP–OES, inductively coupled plasma optical emission spectroscopy; LRE, rare earth elements from La to Gd; REE, rare earth element; TERENO, Terrestrial Environmental Observatories.

on general element content in soils (Kabata-Pendias and Szteke, 2015), there is still a lack of understanding of the detailed links among soil chemical and physical properties, biogeochemical and hydrological processes, and a full spectra of spatial and temporal variations of elements that are affected by and participate in these processes on the catchment scale. The main reasons are the high costs of the experimental setups and labor requirement to perform such intensive studies. Investigations are currently being performed to document biogeochemical and hydrological processes at several long-term ecological research sites such as the HOBE Hydrological Observatory in Denmark (Jensen and Illangasekare, 2011) and the Critical Zone Observatory (Anderson et al., 2008). However, comprehensive datasets are still limited to establish spatially resolved interrelations between biogeochemical properties and processes (Groffman et al., 2009; Schmidt et al., 2011; Yu et al., 2014).

Within the framework of TERENO (Terrestrial Environmental Observatories, http://teodoor.icg.kfa-juelich.de/overview-en?set_language=en), a network of integrated observation platforms has been established in Germany to investigate the consequences of global change for terrestrial ecosystems (Bogena et al., 2010, 2015; Zacharias et al., 2011). The research activities on these long-term (>15 yr) experimental sites include analyses of system state such as soil moisture and temperature, and the fluxes of water, matter, and energy within the continuum of the groundwater-soil-vegetation-atmosphere system, as well as long-term changes of the composition and functioning of microorganisms, plants, and fauna (Bogena et al., 2015). To do so, networks of highly spatially resolved monitoring locations have been set up to provide adequate resolution for documenting the dynamics of the involved processes (Bogena et al., 2015). In addition, integrated mathematical model systems are developed and applied to derive more efficient prevention, mitigation, and adaptation strategies (Bogena et al., 2015).

As an example, the Wüstebach catchment, one of the TERENO observatories located in Western Germany, has been comprehensively documented for site-specific information including biogeochemical, hydrological, and meteorological states and fluxes (Kunkel et al., 2013; Bogena et al., 2015). A comprehensive dataset consisting of hydrological and geochemical measures with high spatial resolution has previously been made available to the public, providing insights into the biogeochemical status of soils in this forested headwater catchment (Wiekenkamp et al., 2016a). It is one of the first three-dimensional representations of biogeochemical soil parameters on the catchment scale. The dataset includes 13 major nutrient concentrations, three soil physical properties, and general soil descriptions at 155 sampling locations in the catchment (Wiekenkamp et al., 2016a).

In this study, we focus on a three-dimensional distribution of additional 39 elements, not only nutrients, but also heavy metals including rare earth elements (REEs), at the same sampling locations to furnish the whole picture of the state and fluxes of the catchment. With the element concentrations provided in the dataset, it is possible to explore the linkage between subsurface chemical variability and geological characteristics, such as the proximity to the stream and the degree of the hill slope. In addition, the present dataset can be combined with that of Wiekenkamp et al. (2016a), for instance, to interpret relationships between element translocation and soil physical and chemical parameters and to illustrate soil nutrient (e.g., Fe) pools and elemental stocks. Moreover, the dataset can be linked with other long-term environmental observation data such as hydrological and meteorological data to help explain element cycling within the catchment. In Supplemental Table S1, we give a list of the analysis activities that have been performed in the catchment for users of the dataset to obtain an overview of possible ways to use the dataset and these measurements. A detailed description of these measurements is provided by Bogena et al. (2015) and the references in Supplemental Table S1. Datasets of relevant studies of the TERENO projects can be found in TERENO Discovery Data Portal (http://teodoor.icg.kfa-juelich.de/ibg-3searchportal2/index.jsp).

# Dataset Description

## Sampling Sites

The studied experimental test site has been described in details in previous publications (Bogena et al., 2015; Gottselig et al., 2017). Briefly, the sampling sites are located within the Wüstebach catchment, Germany, which is part of the Eifel/Lower Rhine Valley Observatory in the TERENO network. The catchment has been intensively studied over the last decade with regard to its hydrological, biogeochemical, and meteorological properties (Bogena et al., 2015), to understand, for instance, the spatiotemporal characteristics of soil moisture and temperature via the SoilNet network (Bogena et al., 2010), and to reveal the spatiotemporal dynamics of discharge, dissolved organic matter, and nitrate in stream (Graf et al., 2014; Bol et al., 2015; Weigand et al., 2017). The setup has also provided new insights into the spatial distribution of P-containing nanoparticles and colloids in the stream (Gottselig et al., 2014), the spatial variability in nitrous oxide emission potential (Liu et al., 2016), and the spatiotemporal variability in preferential flow occurrence (Wiekenkamp et al., 2016c).

In the riparian region of the Wüstebach catchment, the soils are classified as Gleysols and Histosols according to the World Reference Base (IUSS Working Group, 2006), whereas on the upslope of the catchment and away from the stream, the soils are characterized as Cambisols and Planosols. The soils typically have a silty clay loam texture with occasional sandstone inclusions (Richter and Pütz, 2009). The climate of the region is mild humid with a mean annual precipitation of 1200 mm (Bogena et al., 2010) and a mean annual temperature of 7°C (Zacharias et al., 2011).

In late summer (August–September) of 2013, ~8.6 ha of spruce trees [*Picea abies* L. and *Picea sitchensis* (Bong.) Carrière, planted ~1948] were logged (97% of the forest biomass; Etmann, 2009) close to the stream (22.3% of the catchment forestation) to allow for natural regeneration of beech (*Fagus* spp.) forest. The management practice, combined with the unique continuous monitoring setup, revealed new insights related to effects of the deforestation on spatiotemporal hydrological fluxes in the catchment (Wiekenkamp et al., 2016b) and on the transport of sulfate in stream, groundwater, and in the soils (Golor, 2016). The collection of the soil samples for the present dataset was performed before the deforestation, thus providing information on the soil state before the disturbance.

## Sampling Campaign

As previously described (Gottselig et al., 2017), the sampling of the soils was performed between 24 and 27 June 2013. The sampling locations were mainly assigned to the existing points of a wireless soil sensor network that were set up to support geostatistical analysis (SoilNet, 144 locations; Bogena et al., 2010; Rosenbaum et al., 2012). Ten additional locations were assigned to form five equally spaced transects through the catchment (Fig. 1). Half of the SoilNet sampling points were arranged on a 60-m × 60-m grid, whereas the rest SoilNet points were randomly distributed within the grid to also sample small-scale variability (Rosenbaum et al., 2012).

A metal frame of 40 × 40 × 30 cm was forced into the ground. Within the metal frame the bulk samples of the litter and fermented litter layers (L/Of) and the humus-rich horizon (Oh) were collected in bags, respectively. After the complete removal of the L/Of and Oh horizons, two soil cores of 30 cm depth, including the A horizon and part of the B horizon, were taken from the top of the organic-rich mineral layer (A) using a punch-core sampler (HUMAX, Martin Burch AG). Apart from the cores, the remaining soil material from the A horizon was collected in bags. Subsequently, another two 30-cm soil cores were taken directly below the first two cores, resulting in two individual cores containing material of the B or B/C horizon. In the Histosol region close to the source area of the stream, where the soils were extremely wet, two 30-cm soil cores were extracted using a peat sampler (location 501 and 502, H horizon; Fig. 1) or a soil auger (Eijkelkamp) to sample liners down to 1-m depth (location 50 and 450).

All samples were immediately labeled and digitally registered using barcodes following ISO9001 quality management guidelines. After being labeled, the samples were kept at 4°C in a trailer at the sampling field and then stored at −18°C in freezing

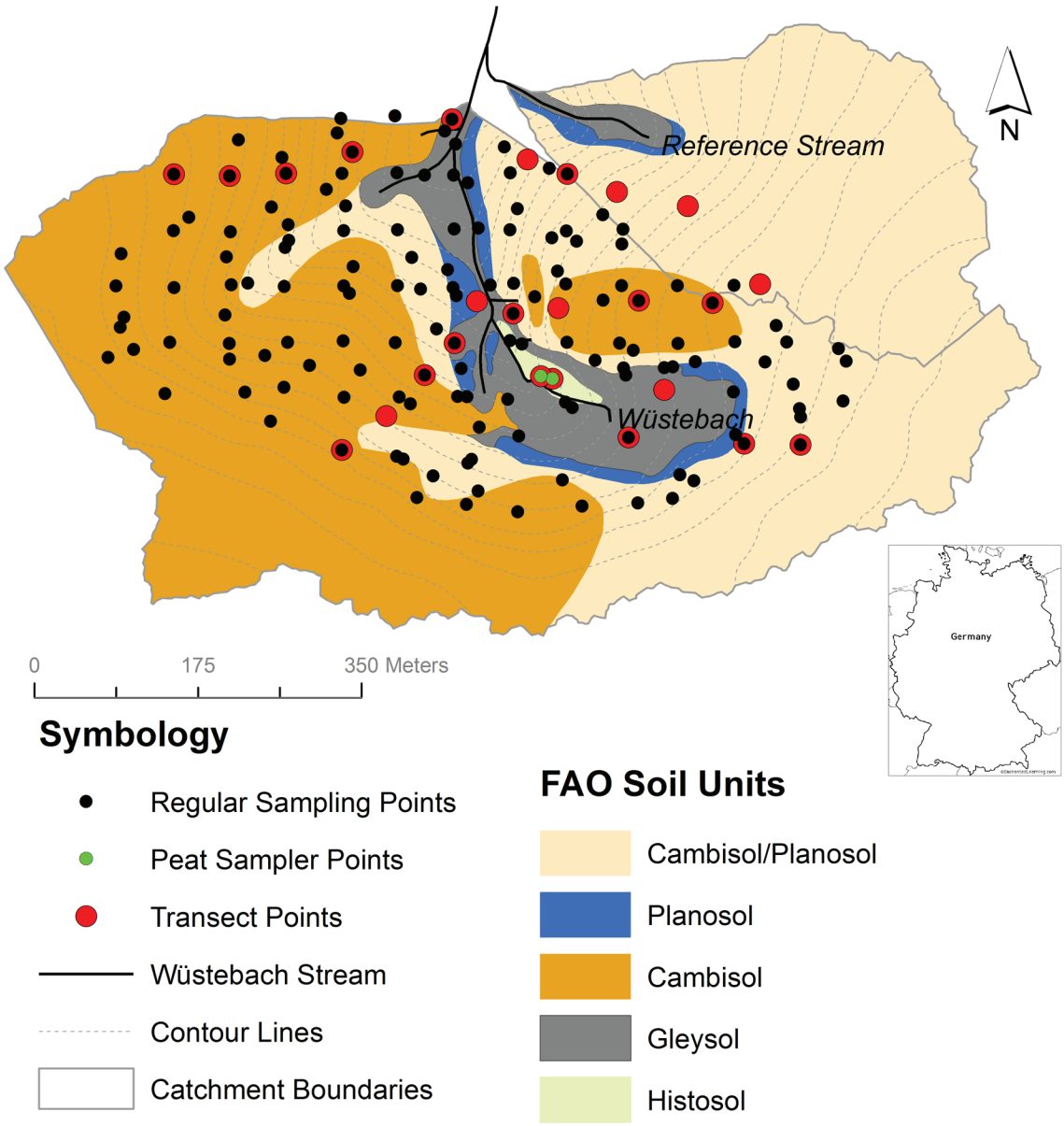


**Fig. 1. Distribution of soil sampling locations in the Wüstebach catchment, adjusted from Richter (2008); resolution of the soil map: 1:2500. Note that the reference stream is currently purely for discharge quantity and quality reference measurements in the catchment. It does not have a specific relevance for the present dataset.**

containers at Forschungszentrum Jülich. These soil samples were later subjected to analyses with respect to soil bulk density, soil texture, pH, water content, carbon and nitrogen contents, and concentrations of manganese, iron, potassium, sulfur, and calcium in soil extractions (Wiekenkamp et al., 2016a). For elemental analysis in the present work, soils of L/Of, Oh, and A horizons collected in bags and B horizons in one of the two upper cores were used. Note that not all sampling locations had a clear sequence of the four representative soil horizons (L/Of, Oh, A, B); therefore, horizons and their respective thickness are given specifically according to each location in the dataset. For sampling locations close to the source area (Histosol region, eight sampling locations), the A horizon was in most cases replaced by an H horizon.

## Sample Preparation and Concentration Determination

Soil samples of each horizon were homogenized by hand in individual bags. The samples were air dried and then passed through a 2-mm sieve. Subsamples of 2 g were weighed for each horizon and extracted with 50 mL aqua regia by a certified commercial laboratory (Landwirtschaftliches Labor Dr. Janssen GmbH), which is accredited according to DIN EN ISO/IEC 17025:2005. Since no certified reference material was available for soils with values for aqua regia extraction at the time of the sample preparation, an in-house standard for aqua regia extraction of soils from the certified laboratory was run together with the samples. The validation of the extraction procedure was performed by analyzing element concentrations in the standard by inductively coupled plasma optical emission spectroscopy (ICP–OES). Aliquots of the extracted solutions were then diluted with Milli-Q water (18.2Ω, Merck Millipore) and analyzed by either inductively coupled plasma mass spectrometry (ICP–MS, Thermo Scientific X Series 2) or ICP–OES (Thermo Scientific iCAP 7400) according to their natural abundance in common soils (Kabata-Pendias and Mukherjee, 2007) at Plymouth University. To eliminate possible spectral interferences of the analytes, a collision/reaction cell was in operation in the ICP–MS, where 7% $H_2$ in He was used as the reaction/collision gas. Platinum was used as the internal standard at a concentration of 10 mg $L^{-1}$ to account for changes in nebulization efficiency and any instrumental drift, with the latter also being monitored by the analysis of check standards every 10 to 15 samples. To evaluate analytical repeatability, ~20 samples were taken out randomly and reanalyzed on different days and by different analysts. It was showed that the repeatability was typically between 2 and 10%, depending on the element and concentration of the element. The elements P, Ca, and S were independently analyzed by both Landwirtschaftliches Labor Dr. Janssen GmbH (Wiekenkamp et al., 2016a) and Plymouth University (the present study), and the difference between the values from the two laboratories was generally within 10%. Users of our dataset can refer to the dataset by Wiekenkamp et al. (2016a) if these elements are needed. Table 1 gives a summary of the analyzed elements in the present study, the corresponding analytical methods, and the detection limits equivalents for solid fractions (μg element $g^{-1}$ soil, dry weight). The elements of interest included (i) essential nutrients for plants (Na, Mg, Mn, Fe, Cu, Zn, and Mo), (ii) light elements (density $\leq$ 5 g $cm^{-3}$: Al, Se, Rb, and Ba), (iii) heavy metals and metalloids (density > 5 g $cm^{-3}$: Cr, Co, Ni, Ga, As, Ag, Cd, Sb, Hg, Tl, Pb, and U), and (iv) REEs (Sc, Y, La, Ce, Pr, Nd, Sm, Eu, Gd, Tb, Dy, Ho, Er, Tm, Yb, and Lu). All analyses were conducted under ISO 9001:2008 certification.

## Dataset Format

Elemental concentrations (mg $kg^{-1}$ dry soil) associated with their respective sampling locations and soil horizons are summarized in a table format in an Excel file and can be downloaded from http://teodoor.icg.kfa-juelich.de/ibg3searchportal2/dispatch?searchparams=freetext-Wuestebach&metadata.detail.view.id=7d37ae00-20f6-408e-8660-33bfba07c869 (Wu et al., 2017). In total, 621 data points per element describe both

**Table 1. List of the analyzed elements, the analytical methods, and the detection limit equivalents for solid fractions ($LOD_{solid}$).**

| Category | Element | Analytical method† | $LOD_{solid}$ |
|---|---|---|---|
| | | | μg $kg^{-1}$ |
| Essential nutrients | Na | ICP–OES | 65,500 |
| | Mg | ICP–OES | 163 |
| | Mn | ICP–OES | 100 |
| | Fe | ICP–OES | 600 |
| | Cu | ICP–OES | 563 |
| | Zn | ICP–OES | 150 |
| | Mo | ICP–MS | 17.9 |
| Light elements | Al | ICP–OES | 2,380 |
| | Se | ICP–MS | 55 |
| | Rb | ICP–MS | 2.88 |
| | Ba | ICP–OES | 150 |
| Heavy metals and metalloids | Cr | ICP–OES | 425 |
| | Co | ICP–MS | 1.63 |
| | Ni | ICP–OES | 425 |
| | Ga | ICP–MS | 1.25 |
| | As | ICP–MS | 8.88 |
| | Ag | ICP–MS | 52.5 |
| | Cd | ICP–MS | 2.50 |
| | Sb | ICP–MS | 2.50 |
| | Hg | ICP–MS | 33.8 |
| | Tl | ICP–MS | 1.13 |
| | Pb | ICP–OES | 3,130 |
| | U | ICP–MS | 1.50 |
| Rare earth elements (REEs) | Sc | ICP–MS | 9.13 |
| | Y | ICP–MS | 0.25 |
| | La | ICP–MS | 0.25 |
| | Ce | ICP–MS | 3.75 |
| | Pr | ICP–MS | 0.125 |
| | Nd | ICP–MS | 0.125 |
| | Sm | ICP–MS | 0.125 |
| | Eu | ICP–MS | 0.125 |
| | Gd | ICP–MS | 0.375 |
| | Tb | ICP–MS | 0.125 |
| | Dy | ICP–MS | 0.125 |
| | Ho | ICP–MS | 0.125 |
| | Er | ICP–MS | 0.125 |
| | Tm | ICP–MS | 0.125 |
| | Yb | ICP–MS | 0.125 |
| | Lu | ICP–MS | 0.125 |

† ICP–OES, inductively coupled plasma optical emission spectroscopy ; ICP–MS, inductively coupled plasma mass spectrometry.

horizontal and vertical distributions of various elements within the catchment area. The dataset is sorted first according to the SoilNet locations, followed by the transect locations, so that the element distribution per profile can be clearly seen for each location. The present dataset is based on the same soil samples in the previous studies of physical and chemical soil properties by Wiekenkamp et al. (2016a). Therefore, the descriptions of detailed soil profile and soil texture and the determination of soil physical and chemical parameters by Wiekenkamp et al. (2016a) can be used for the present dataset. It is important to note that, in the present dataset, the concentrations of the essential nutrients Fe, Mn, and Na in soils are based on the more extensive extraction of the soils by aqua regia, rather than by $CaCl_2$–DPTA extraction, as shown in the previous study (Gottselig et al., 2017), which was used to solely estimate the Fe bound to organic matter.

## Major Characteristics of the Dataset

The dataset describes the spatial distribution of the concentration of 39 elements in the sampled soils, including plant essential and beneficial nutrients, heavy metals and metalloids, some of which are usually studied as environmental pollutants, as well as the REEs whose oxides are used as tracers to determine erosion. In this section, we provide general description for each of these element groups using exploratory data analysis and geostatistical methods. Selenium, Al, Pb, and Ce were selected from each group, because (i) Se and Pb are of wide interest in nutrition and pollution studies, respectively; (ii) Al is highly relevant to the catchment because the soils have very low pH values; and (iii) Ce is the most abundant REE, and its distribution in soil profile and across the catchment is representative of the REEs. To demonstrate relative vertical abundance of each element, boxplots were generated using individual horizon data (Fig. 2). The H horizon of the sampling location close to the stream source was separated from the A horizon of other locations in the boxplots to explore whether elemental concentration at these areas were affected by high soil water content. The significance of differences between horizons was assessed by performing one-way ANOVA in OriginPro (V. b9.2.272; OriginLab, 2015). To investigate the spatial distribution of the elements within the catchment area, kriging was used for each horizon (Fig. 3). It is important to note that the H horizons were grouped within the distribution map of the A horizons, since the H horizons were present at these locations instead of A horizons. In addition, these H horizons had similar depth to the A horizons at other locations and had an Oh horizon overlying them and a B horizon below them. Using kriging, values at unsampled locations were predicted according to spatial dependence among sampled locations (Goovaerts, 1998). We used the approach used by Gottselig et al. (2017) and generated experimental semivariograms by calculating the semivariance [$\gamma(h)$] using:

$$\gamma(h) = 0.5N(h)\sum_{\alpha=1}^{N(h)}\left[z(u_\alpha) - z(u_\alpha + h)\right]^2$$

where $N$ is the number of pairs, and $z(u_\alpha) - z(u_\alpha + h)$ describes the difference between a pair within a given distance class ($h$) (Goovaerts, 1998). Before the calculation of the semivariogram, concentration data of some elements (here, Pb in the four horizons and Al in the L/Of horizon, Fig. 3) were logarithmically transformed to normalize their distributions. Manual fitting of exponential semivariograms and ordinary kriging were performed using the automap package (Hiemstra et al., 2009) in R (V. 3.3.2, R Core Team, 2016). In the end, the generated ASCII files were imported into ArcGIS (V. 10.3; ESRI, 2014) for further visualization.

## Plant Essential and Beneficial Nutrients

The concentrations of essential cationic macronutrients (e.g., Mg), micronutrients (e.g., Zn), and beneficial nutrients (e.g., Se) for plants were determined in the sampled soil profiles. Anionic nutrients, such as P and S, were already provided in the dataset of Wiekenkamp et al. (2016a), which can be combined with the present dataset to provide an overview on the nutritional level of the catchment area as a whole. In addition, by combining the element concentrations provided in the present dataset and the soil depth and bulk density in the dataset of Wiekenkamp et al. (2016a), one can use the dataset to estimate the element stocks in the soil.

The vertical distribution pattern of the nutrients is related to their abundance in soils. The median concentration of abundant elements such as Fe, Mn, and Mg, increased with depth, where the mineral horizons account for at least 70% of the total concentration in the whole profile. However, the concentrations of trace elements such as Cu, Mo, and Se (Fig. 2a) decreased with depth, with the organic layers (fresh litter layer and fermented litter layer) containing up to 48% of the total concentration. The peak concentrations of Cu and Se were found in the H horizons close to the stream source. Notably, the Se concentrations in the Wüstebach catchment were higher than the world average value (0.33 mg $kg^{-1}$) but were still consistent with previous research reporting that the surface layer of forest soils generally has a higher content of Se (Kabata-Pendias and Mukherjee, 2007). As the soil pH values in this catchment are generally very low (between 2.5 and 4.0; Wiekenkamp et al., 2016a), Al, a beneficial element to some plant species (Osaki et al., 1997), is one of the elements whose mobility can be significantly affected. The median concentration of Al in the Wüstebach catchment increased with depth, with majority of Al stored in the mineral horizons. It is worth noting that the clear-cut of the spruce trees in late summer 2013 (after the collection of the soil samples for the present dataset) may have an effect on the soil pH values and thus concentrations and motilities of the elements such as Al and Fe, which are pH sensitive.

## Heavy Metals and Metalloids

In this dataset, we also analyzed several heavy metals and metalloids that are considered by many authors to be environmental pollutants (e.g., Pb, Cd, and As). The depth distribution of these elements generally showed two distinct patterns. Whereas the concentrations of Co, Cr, Ga, Ni, and U increased with depth, showing lithospheric characteristics, the median concentrations of Hg, Ag, As, Cd, Pb, Sb, and Tl, in contrast, were higher in the surface organic-rich horizons and underlying A horizons compared with the deeper B horizons. For instance, the median concentration of Pb in the Oh horizon was more than five times than that measured in the B horizon. The data distribution of these elements within the catchment area was more diverse in the L/

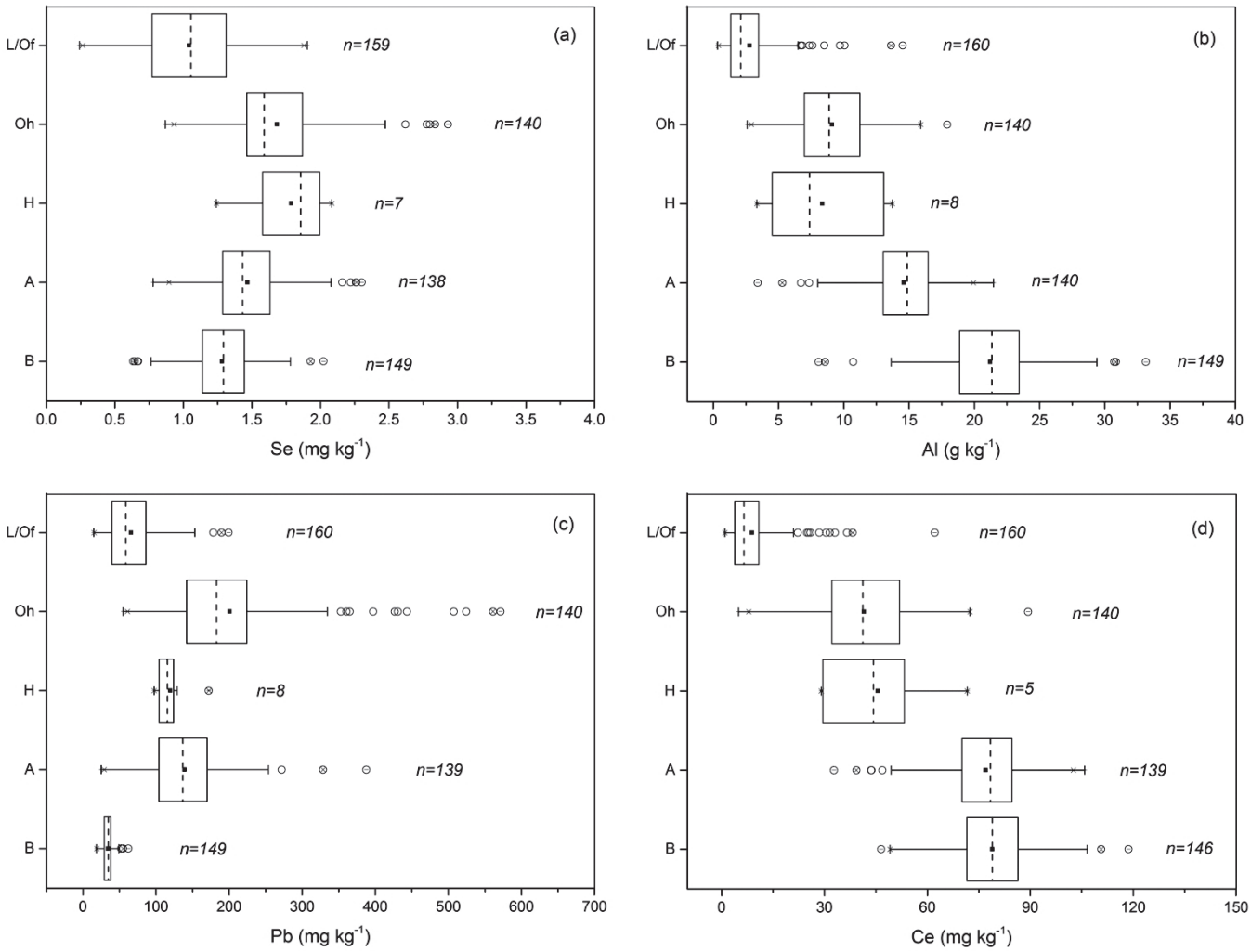


**Fig. 2. Boxplots showing depth-profile of (a) Se, (b) Al, (c) Pb, and (d) Ce in the Wüstebach catchment. One-way ANOVA was performed, showing significant differences among horizons at the 0.001 level for all the four elements. Notice that *n* values per horizon are given; most data is available for L/Of, Oh, A, and B horizons. Extreme outliers were identified in R by setting the upper and lower limits as three times the inter-quartile range above or below the upper and lower quartile range, respectively.**

Of, Oh, and A horizons, whereas the concentrations were within limited ranges in the B horizons. In contrast, elements with lithospheric characteristics generally showed a larger concentration range among the sampled locations in deeper horizons than in the organic-rich horizons, indicating the heterogeneity of the parent materials.

## Rare Earth Elements

Rare earth elements include 17 elements (i.e., the 15 elements of lanthanides, as well as Sc and Y). Due to the fact that they exhibit similar chemical properties, these 17 elements are generally studied together. With respect to density, the REEs are categorized as heavy metals. As in nature Pm is present only in trace amounts and radioactive, it was not analyzed in the present study. In terrestrial systems, the contents of the REEs (here, the lanthanides) decrease with an increase of their atomic number and follow the Oddon–Harkins rule stating that an element with an even atomic number is more abundant than the neighboring element with an odd atomic number (Kabata-Pendias and Mukherjee, 2007). Our present dataset clearly confirmed this peculiarity, where Ce (atomic number 58) (Fig. 2d) was the most abundant in the sampled soils, and Lu (atomic number 71) was the least abundant. The higher concentrations of the REEs were nearly exclusively found in the mineral horizons in the catchment. However, the REEs concentrations in the Oh horizons were generally higher than in the fresh litter horizons, indicating that organic compounds derived from litter decomposition played an important role in the distribution of the REEs (Kabata-Pendias and Mukherjee, 2007). The temporal and spatial distribution of the REEs in soils can be used as tracers for the study of soil erosion processes (see review paper by Zhu et al., 2010).

## Spatial Distribution

The present dataset consists of >600 data points collected at highly spatially resolved sampling locations, providing information on the concentration distributions of four key soil horizons for each element. From these data points, one can reconstruct a three-dimensional elemental distribution within the catchment. For many elements we studied, the spatial distribution patterns on individual horizons showed close relationships with the proximity to the stream (such as Tl, Cu, and Co), whereas others showed a distinct distribution pattern on the two sides of the steam, which were related to soil types (like Lu and U).

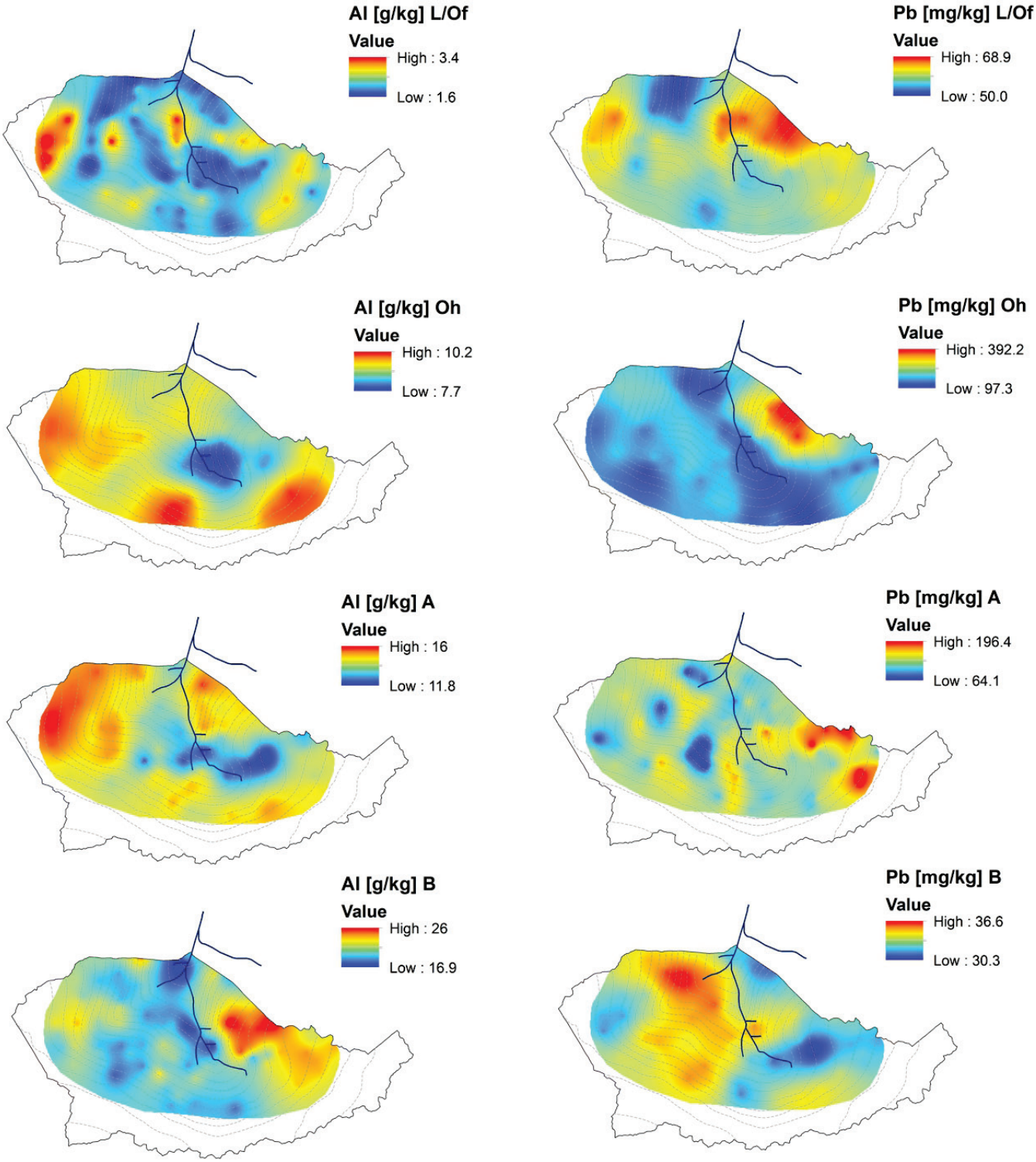


**Fig. 3. Spatial distribution of Al (left) and Pb (right) in the catchment area for the four principle soil horizons (L/Of, Oh, A, and B, top to bottom rows) using ordinary kriging. Notice that the individual legend for each horizon for Al and Pb concentration distributions. Concentration data of Pb (all four horizons) and Al (L/Of horizon) were logarithmically transformed before the calculation of the semivariogram. Extreme outliers were identified in R by setting the upper and lower limits as three times the inter-quartile range above or below the upper and lower quartile range, respectively.**

To provide an example, we used ordinary kriging to obtain spatial maps for Al and Pb (Fig. 3) and to illustrate their distribution pattern for the individual horizons across the catchment area. Separate variogram models were fitted for each individual soil horizon, and individual maps were generated for the four dominant horizons (L/Of, Oh, A, and B). Note that the H horizons at the stream source were presented in the distribution map of the A horizon. The overall Al concentration increased with the depth as observed in the boxplots. In all the four main horizons, lower Al concentrations were found in the riparian zone near the Wüstebach stream. Furthermore the Al concentrations in the L/Of, Oh and A horizons were found to be the lowest in the stream source region. However, the B horizon of the central and the lower part of the Wüstebach catchment exhibited

the lowest Al concentration. The highest Al concentration was found on the upslope of the east side of the stream in the B horizon, whereas the A horizon of this side did not show a particularly high amount of Al. In contrast, the upslope on the west side away from the stream showed similar concentrations in both A and B horizons. The areas with hotspots (relatively high Al concentration) in the Oh horizon were clearly linked to the high Al concentrations in the A horizon.

For Pb, however, surface soil layers had a considerably higher overall Pb concentration than the deeper B horizons. In addition, in these highlighted horizons Pb seemed to be higher on the east upslope of the catchment, whereas in the B horizons, Pb was more abundant on the west upslope. However, Pb concentrations in the B horizon showed a limited range across the catchment. Our results suggested that Pb in the Wüstebach catchment might not have originated from the parent material but derived from other sources, such as forest litter, and accumulated in the Oh horizons over the years with a subsequent downward movement trend into the A horizons.

### Correlations among Elements

The large number of data points in our dataset allowed us to investigate interrelations among the elements on the catchment scale. In addition, correlations of soil chemical properties provided in this study and our previous dataset can be established. Here, as an example, we explored the Pearson correlation coefficient between every two elements that we analyzed using all the data from the four dominant horizons (Supplemental Table S2). The REEs showed significant positive linear correlations with each other with the coefficients $\rho > 0.73$. The general trend for the lanthanides was the closer their atomic numbers, the closer the linear relationship between the two. However, a better coefficient was found between Y and the HREs (second group of the REEs from Tb to Lu) than Y and the LREs (first group of the REEs from La to Gd). The coefficients between Sc and the rest of REEs were similar ($0.73 < \rho < 0.83$). In addition, U had a highly positive linear correlation with the REEs, especially with the HREs ($\rho > 0.9$). Other elements that showed highly positive linear coefficients with the REEs were Mg, Fe, Al, Rb, Cr, Co, Ni, and Ga, all of which were abundant in the mineral horizons. Moreover, these elements also showed good positive linearity between each other. Additionally, Mo, Sb, Ag, and Pb were well correlated with each other ($\rho > 0.68$).

## Summary

The present dataset on elemental concentrations of both plant nutrients and other metals and metalloids in soils was based on the analyses of a large number of samples that were highly spatially resolved in a catchment located in western Germany. It provided a three-dimensional view of elements reflecting natural soil development of a forested ecosystem on the catchment scale. Investigating the vertical and lateral distribution of individual elements, exploring the interrelationship among the elements, and linking the present dataset and others (Wiekenkamp et al., 2016a) will provide insights into elemental cycling in terrestrial and aquatic ecosystems. Future research may involve temporal distribution of these elements and other soil chemical and physical properties to facilitate the understanding of management- and climate-induced changes on catchment processes and responses.


### Acknowledgments

We gratefully acknowledge the immense support of Odilia Esser, Rainer Harms, Claudia Walraf, Anne Berns, Anna Missong, and Nils Borchard and the complete IBG-3 soil sampling team. Additionally, we wish to acknowledge the TERENO project funded by the Helmholtz Association of German Research Centers, which provided financial support for this project.


### Data Citation


Wu, B., I. Wiekenkamp, Y. Sun, A.S. Fisher, R. Clough, N. Gottselig, H. Bogena, T. Pütz, N. Brüggemann, H. Vereecken, and R. Bol. 2017. A dataset for three-dimensional distribution of 39 elements including plant nutrients and other metals/metalloids in the soils of a forested headwater catchment. http://teodoor.icg.kfa-juelich.de/ibg3searchportal2/dispatch?searchparams=freetext-Wuestebach&metadata.detail.view.id=7d37ae00-20f6-408e-8660-33bfba07c869. TERENO Project 7d37ae00-20f6-408e-8660-33bfba07c869.


### References


Anderson, S.P., R.C. Bales, and C.J. Duffy. 2008. Critical zone observatories: Building a network to advance interdisciplinary study of Earth surface processes. Mineral. Mag. 72:7–10. doi:10.1180/minmag.2008.072.1.7

Bogena, H.R., R. Bol, N. Borchard, N. Brüggemann, B. Diekkrüger, C. Drüe et al. 2015. A terrestrial observatory approach for the integrated investigation of the effects of deforestation on water, energy, and matter fluxes. Sci. China Earth Sci. 58:61–75. doi:10.1007/s11430-014-4911-7

Bogena, H.R., M. Herbst, J.A. Huisman, U. Rosenbaum, A. Weuthen, and H. Vereecken. 2010. Potential of wireless sensor networks for measuring soil water content variability. Vadose Zone J. 9:1002–1013. doi:10.2136/vzj2009.0173

Bol, R., A. Lücke, W. Tappe, S. Kummer, M. Krause, S. Weigand et al. 2015. Spatio-temporal variations of dissolved organic matter in a German forested mountainous headwater catchment. Vadose Zone J. 14(4):1–12. doi:10.2136/vzj2015.01.0005

ESRI. 2014. ArcGIS desktop: Release 10.3. Envion. Syst. Res. Inst., Redlands, CA.

Etmann, M., editor. 2009. Dendrologische aufnahmen im Wassereinzugsgebiet Oberer wüstebach anhand verschiedener mess- und schätzverfahren. (In German.) Univ. Münster, Münster, Germany.

Golor, T. 2016. Spatial and temporal stream, groundwater, and soil sulfate distributions influenced by a partial deforestation at the experimental test site Wüstebach, Eifel (Germany). Master's thesis, Univ. of Bonn, Bonn, Germany.

Goovaerts, P. 1998. Geostatistical tools for characterizing the spatial variability of microbiological and physico-chemical soil properties. Biol. Fertil. Soils 27:315–334. doi:10.1007/s003740050439

Gottselig, N., I. Wiekenkamp, L. Weihermüller, N. Brüggemann, A.E. Berns, H.R. Bogena et al. 2017. A three-dimensional view on soil biogeochemistry: A dataset for a forested headwater catchment. J. Environ. Qual. 46:210–218. doi:10.2134/jeq2016.07.0276

Gottselig, N., R. Bol, V. Nischwitz, H. Vereecken, W. Amelung, and E. Klumpp. 2014. Distribution of phosphorus-containing fine colloids and nanoparticles in stream water of a forest catchment. Vadose Zone J. 13. doi:10.2136/vzj2014.01.0005

Graf, A., H.R. Bogena, C. Drüe, H. Hardelauf, T. Pütz, G. Heinemann, and H. Vereecken. 2014. Spatiotemporal relations between water budget components and soil water content in a forested tributary catchment. Water Resour. Res. 50:4837–4857. doi:10.1002/2013WR014516

Groffman, P.M., K. Butterbach-Bahl, R.W. Fulweiler, A.J. Gold, J.L. Morse, E.K. Stander et al. 2009. Challenges to incorporating spatially and temporally explicit phenomena (hotspots and hot moments) in denitrification models. Biogeochemistry 93:49–77. doi:10.1007/s10533-008-9277-5

Hiemstra, P.H., E.J. Pebesma, C.J.W. Twenhöfel, and G.B.M. Heuvelink. 2009. Real-time automatic interpolation of ambient gamma dose rates from the Dutch Radioactivity Monitoring Network. Comput. Geosci. 35:1711–1721. doi:10.1016/j.cageo.2008.10.011

IUSS Working Group. 2006. World reference base for soil resources. World Soil Resour. Rep. 103. FAO, Rome.

Jensen, K.H., and T.H. Illangasekare. 2011. HOBE: A hydrological observatory in Denmark. Vadose Zone J. 10:1–7. doi:10.2136/vzj2011.0006

Kabata-Pendias, A., and A.B. Mukherjee. 2007. Trace elements from soil to human. Springer-Verlag, Berlin, Heidelberg. doi:10.1007/978-3-540-32714-1

Kabata-Pendias, A., and B. Szteke. 2015. Trace elements in abiotic and biotic environments. CRC Press, Boca Raton, FL. doi:10.1201/b18198

Kunkel, R., J. Sorg, O. Kolditz, K. Rink, J. Klump, R. Gasche, and F. Neidl. 2013. TEODOOR: A spatial data infrastructure for terrestrial observation data. In: Proceedings of the 10th IEEE International Conference on Networking, Sensing and Control (ICNSC), Evry, France. 10–12 Apr. 2013. IEEE Xplore. p. 242–245. doi:10.1109/ICNSC.2013.6548744

Liu, S., M. Herbst, R. Bol, N. Gottselig, T. Pütz, D. Weymann et al. 2016. The contribution of hydroxylamine content to spatial variability of $N_2O$ formation in soil of a Norway spruce forest. Geochim. Cosmochim. Acta 178:76–86. doi:10.1016/j.gca.2016.01.026

OriginLab. 2015. OriginPro. Release b9.2.272. OriginLab, Northampton, MA.

Osaki, M.T., T. Watanabe, and T. Tadano. 1997. Beneficial effect of aluminum on growth of plants adapted to low pH soils. Soil Sci. Plant Nutr. 43:551–563. doi:10.1080/00380768.1997.10414782

R Core Team. 2016. R: A language and environment for statistical computing. R Foundation for Statistical Computing, Vienna, Austria.

Richter, F. 2008. Soil map for site-specific investigation: Procedure for the source area of the Wüstebach Valley (Forest). (In German.) Geol. Survey North Rhine-Westphalia, Krefeld, Germany.

Richter, F., and T. Pütz. 2009. Bodenkundliche untersuchungen für biotopmanagement und grundlagenforschung im nationalpark Eifel. In: Jahrestagung der Deutschen Bodenkundlichen Gesellschaft: Böden—eine endliche ressource. (In German.) Univ. Bonn, Bonn, Germany. p. 79–88. https://www.dbges.de/de/system/files/mitteilungen_dbg/Bd112.pdf (accessed 15 Sept. 2017).

Rosenbaum, U., H.R. Bogena, M. Herbst, J.A. Huisman, T.J. Peterson, A. Weuthen et al. 2012. Seasonal and event dynamics of spatial soil moisture patterns at the small catchment scale. Water Resour. Res. 48:W10544. doi:10.1029/2011WR011518

Schmidt, M.W.I., M.S. Torn, S. Abiven, T. Dittmar, G. Guggenberger, I.A. Janssens et al. 2011. Persistence of soil organic matter as an ecosystem property. Nature 478:49–56. doi:10.1038/nature10386

Sigel, A., and H. Sigel. 2003. Metal ions in biological systems. Vol. 40: The lanthanides and their interrelations with biosystems. Marcel Dekker, Basel, Switzerland.

Weigand, S., R. Bol, R. Reichert, A. Graf, I. Wiekenkamp, S. Stockinger et al. 2017. Spatio-temporal dependency of dissolved organic carbon to nitrate in stream- and groundwater of a humid forested catchment: A wavelet transform coherence analysis. Vadose Zone J. 16(3):1–14. doi:10.2136/vzj2016.09.0077

Wiekenkamp, I., N. Gottselig, L. Weihermüller, N. Brüggemann, A.E. Berns, H.R. Bogena et al. 2016a. Three dimensional soil biogeochemistry data of a forested catchment (Wuestebach). http://teodoor.icg.kfa-juelich.de/ibg3searchportal2/dispatch?metadata.detail.view.id=e3886301-7252-4142-b1a4-333dfe7f1ca4. TERENO Project. e3886301-7252-4142-b1a4-333dfe7f1ca4.

Wiekenkamp, I., J.A. Huisman, H.R. Bogena, A. Graf, H.S. Lin, C. Drüe, and H. Vereecken. 2016b. Changes in measured spatiotemporal patterns of hydrological response after partial deforestation in a headwater catchment. J. Hydrol. 542:648–661. doi:10.1016/j.jhydrol.2016.09.037

Wiekenkamp, I., J.A. Huisman, H.R. Bogena, H.S. Lin, and H. Vereecken. 2016c. Spatial and temporal occurrence of preferential flow in a forested headwater catchment. J. Hydrol. 534:139–149. doi:10.1016/j.jhydrol.2015.12.050

Yu, X., C. Duffy, J. Kaye, W. Crow, G. Bhatt, and Y. Shi. 2014. Watershed reanalysis of water and carbon cycle models at a critical zone observatory. In: V. Lakshmi, editor, Remote sensing of the terrestrial water cycle. John Wiley & Sons, Hoboken, NJ. p. 493–509, doi:10.1002/9781118872086.ch31.

Zacharias, S., H. Bogena, L. Samaniego, M. Mauder, R. Fuß, T. Pütz et al. 2011. A network of terrestrial environmental observatories in Germany. Vadose Zone J. 10:955–973. doi:10.2136/vzj2010.0139

Zhu, M.-Y., S.-D. Tan, W.-Z. Liu, and Q.-F. Zhang. 2010. A review of REE tracer method used in soil erosion studies. Agric. Sci. China 9:1167–1174. doi:10.1016/S1671-2927(09)60204-2